Proceedings of the 25th International Conference on
Port and Ocean Engineering under Arctic Conditions
June 9-13, 2019, Delft, The Netherlands

Probabilistic peak ice load model

Janne Ranta, Arttu Polojärvi
Aalto University School of Engineering, Department of Mechanical Engineering, Finland

ABSTRACT

This paper summarizes our recent work on mechanisms and limits for the peak ice load values on wide inclined marine structures. The study is based on data from two-dimensional combined finite-discrete element method simulations and introduces a simple probabilistic model, in which the ice failure takes place either by buckling or by local crushing. We demonstrate how the model can be used in the analysis of peak ice load events.

KEY WORDS: Ice loads; FEM-DEM; Modelling.

1. Introduction

The number of marine operations related to transportation, offshore wind energy, and offshore drilling in the Arctic is increasing. A key factor in ensuring the safety and sustainability of these operations is the reliable prediction of sea ice loads, which arise from a complex and stochastic ice-structure interaction process (Sanderson, 1988; Daley et al., 1998; Jordaan, 2001). It has become popular to study ice loads based on rather complicated numerical tools. We believe the true value of the numerical models resides in careful analysis, which yields the actual insight on ice mechanics and makes it possible to conceive reliable ice load models.

Here we introduce a rather simple approach for studying maximum peak ice load events on inclined structures. The introduced model extends our buckling model for peak ice loads (Ranta et al., 2018a). This model assumed that the peak ice load on a structure was limited by force chain buckling (Figure 1) and yielded a maximum peak ice load value

$$F^p = a\sqrt{kEI}, \tag{1}$$

where $a = a(\chi)$ is a buckling-mode-dependent dimensionless multiplier, $k = \rho_w g$ is the specific weight of water (ρ_w is the mass density of water and g the gravitational acceleration), E is

the effective modulus of ice, and $I = h^3/12$ is the second moment of area of a beam having rectangular cross-section, unit width and thickness of h.

The new model has its basis on mechanical behavior of ice while simultaneously being stochastic, hence we call it here a probabilistic limit load model. We believe the probabilistic limit load model is of use in gaining insight for the analysis of ice-structure interaction processes. Here we only briefly demonstrate the capabilities of the model by studying the failure mode of ice in peak ice load events on inclined structure. The work we present here is largely based on Ranta and Polojärvi (2019), where the model is extended into a probabilistic peak ice load algorithm and its results compared to simulation and full-scale data. We start by first describing the FEM-DEM simulations, on which the model is based on and then introduce the model itself.

2. Methods

The model is based on 2D FEM-DEM simulations, performed with an in-house code of Aalto University ice mechanics group. The code is based on the models described in Hopkins (1992) and Paavilainen et al. (2009) and its results validated in Paavilainen et al. (2009) and Paavilainen and Tuhkuri (2012). The ice sheet was formed by discrete elements connected with Timoshenko beams, which were linearly elastic up to a pre-defined failure criterion Schreyer et al. (2006), and then went through an energy dissipating cohesive softening before failure. Discrete elements were used to treat contact interactions between the ice blocks and the ice and the structure.

The model development was based on 350 simulations. Table 1 gives the parameters of the simulations with Table 2 summarizing the seven simulations sets, S1...S7. Each set contained 50 simulations where all parameters were constant, but the initial conditions slightly differed: An initial vertical velocity of the order of 10^{-12} m/s was applied at the free edge of the ice sheet at the start of the simulation (see Ranta et al. (2018b) for details). As shown in Table 2, the simulation sets S1...S6 differed from each other by the values of h and σ_p. Simulation set S7 had thick ice, $h = 1.25$ m, and a high value of 8 MPa for σ_{p}. Simulations within each set, differing by their initial conditions only, produced different ice loading processes (Figure 2).

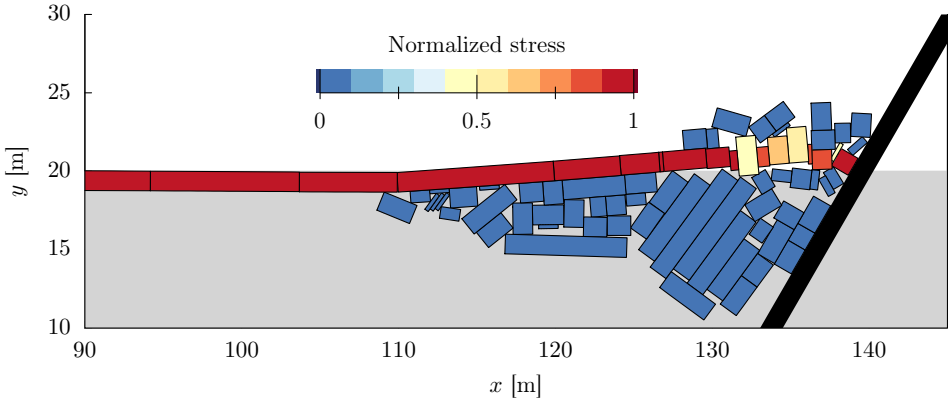

Figure 1: Snapshot from a FEM-DEM simulation showing a force chain, a sequence of ice blocks in contact due to high compressive stress, transmitting the ice load. Colors indicate the average normalized compressive stress on the ice blocks.

Table 1: Main simulation parameters. The parameter values were mostly chosen following Timco and Weeks (2010).

	Description and symbol		Unit	S1...S7
General	Gravitational acceleration	g	m/s^2	9.81
	Ice sheet velocity	v	m/s	0.05
	Drag coefficient	c_d		2.0
Ice	Thickness	h	m	0.5, 0.875, 1.25
	Effective modulus	E	GPa	4
	Poisson's ratio	ν		0.3
	Density	ρ_i	kg/m^3	900
	Tensile strength	σ_f	MPa	0.6
	Shear strength	τ_f	MPa	0.6
Contact	Plastic limit	σ_p	MPa	1.0, 2.0, 8.0
	Ice-ice friction coefficient	μ_{ii}		0.1
	Ice-structure friction coefficient	μ_{iw}		0.1
Water	Density	ρ_w	kg/m^3	1010
Structure	Slope angle	α	deg	70

Table 2: Simulation sets S1...S7 of this study. The able also shows the number N and the indices (ID) of the simulations in each set. More detailed list of simulation parameters is given in Table 1.

Set	IDs	N	h	σ_p
			[m]	[MPa]
S1	1-50	50	0.5	1
S2	51-100	50	0.5	2
S3	101-150	50	0.875	1
S4	151-200	50	0.875	2
S5	201-250	50	1.25	1
S6	251-300	50	1.25	2
S7	301-350	50	1.25	8

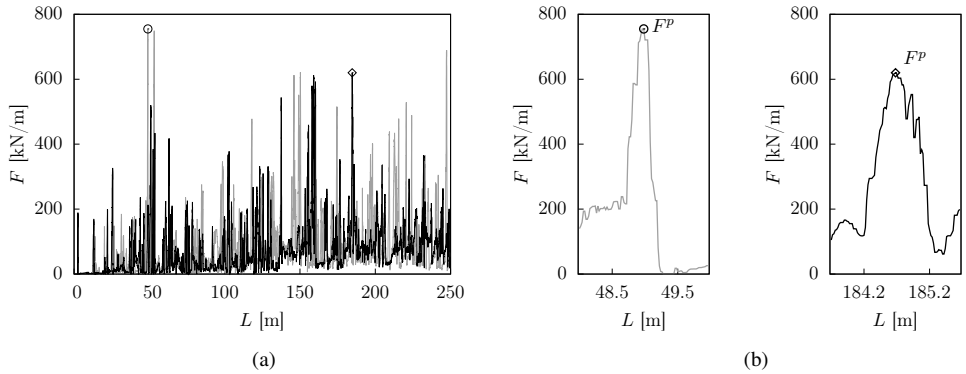

Figure 2: Two ice load F-records from two simulations with same parameterization but different initial conditions: (a) F plotted against length of pushed ice, L, and (b) close-ups of the maximum peak ice load, F^p, events. The value of F^p differs between the simulations. Here the ice thickness $h = 1.25$ m and the plastic limit $\sigma_p = 1$ MP.

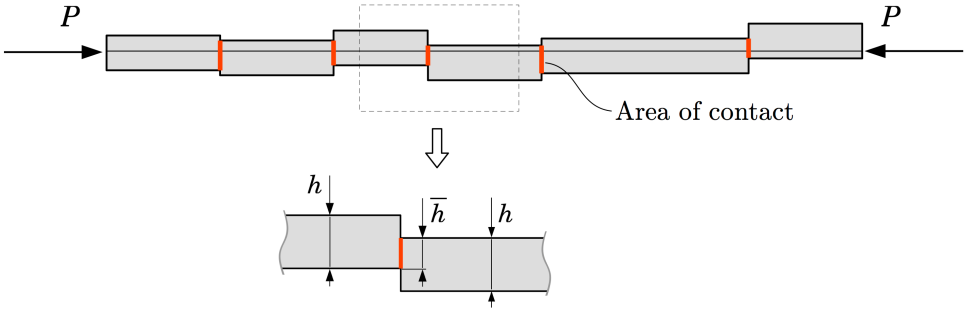

Figure 3: Force chain transmitting a load P and one contact interface between a pair of ice blocks, an elementary unit of the probabilistic limit load model. Blocks are of thickness h and the contact has a length of $\bar{h}$.

The probabilistic limit load model, used below for studying peak ice load events, extends the above-described buckling model by (1) supplementing it with a local crushing model and (2) by accounting for the stochasticity in the contact geometries of the blocks belonging to the force chains. An elementary unit of the model is a contact interface between a pair of ice blocks belonging to a force chain (Figure 3). The blocks are in a partial face-to-face contact due to a compressive load P. Local crushing is assumed to occur at the contact interface if $P \geq \bar{h}\sigma_p$, where $\bar{h}$ is the length of the contact interface and σ_p is the limit for compressive stress.

By using Equation 1 and the criterion $P \geq \bar{h}\sigma_p$ for local crushing, it is simple to determine the critical contact length $\bar{h}_c$, for which the local crushing event occurs with the same compressive load as the buckling. This is given by

$$\sigma_p \bar{h}_c = a\sqrt{kEI} \quad \Rightarrow \quad \bar{h}_c = \frac{a}{\sigma_p}\sqrt{kEI} = \frac{a}{\sigma_p}\sqrt{\frac{\rho_w g E h^3}{12}}. \tag{2}$$

When the contact length $\bar{h} \leq \bar{h}_c$ for a given pair of contacting blocks, then the local crushing event limits the P transmitted by them. In contrast, when $\bar{h} > \bar{h}_c$, buckling limits P.

The contact length $\bar{h}$ and the ice thickness h can be used to introduce a non-dimensional contact offset $e = 1 - \bar{h}/h$. When $e = 0$, the contact length $\bar{h}$ is equal to the ice thickness h. When $e = 1$, the contact length becomes zero and the force chain does not exist. The critical contact offset

e_c (Figure 3), at which the root cause of ice failure changes from buckling to local crushing is then

$$e_c = 1 - \frac{\bar{h}_c}{h} = 1 - \frac{a\sqrt{kEI}}{\sigma_p h} = 1 - \frac{a}{\sigma_p}\sqrt{\frac{\rho_w g E h}{12}}. \tag{3}$$

Using everything above, the maximum load P^m a system with one contact interface is able to transmit can be determined to be

$$P^m = \begin{cases} a\sqrt{kEI} & \text{if } e < e_c \qquad \text{(limiting mechanism: buckling)} \\ \sigma_p h\,(1-e) & \text{if } e \geq e_c. \qquad \text{(limiting mechanism: local crushing).} \end{cases} \tag{4}$$

In a peak load event occurring in an ice-structure interaction process, the e values for the pairs of contacting blocks in force chains vary randomly. The distribution for e values is not known, and thus, a simple triangular distribution that has its maximum at e_m can initially be chosen. This distribution has a cumulative distribution function

$$T(e) = \begin{cases} 0 & , e < 0 \\ (2e_m - e)e/e_m^2 & , 0 \leq e \leq e_m\,, \quad \text{where} \quad 0 < e_m < 1 \\ 1 & , e > e_m. \end{cases} \tag{5}$$

where it is assumed that e can have a random value varying at an interval of $0 \ldots e_m$, where $0 < e_m < 1$. (By definition, e could vary between values 0 and 1, but in the case of value 1, the model occasionally predict the maximum peak ice load to have value 0.) Relating the randomness of the process to parameter e causes the stochasticity of the loads to be related to the geometrical configuration of the rubble pile, which can be justifiably considered to be a random physical property of a system consisting of still intact ice, ice rubble, and an inclined structure.

Triangular cumulative distribution function $T(e)$ leads to fairly simple formulas for the probabilities of buckling and local crushing events. For a pair of contacting blocks and one contact interface, the buckling event limits the load when $e < e_c$. The probability of a buckling event reads

$$p(\text{buckles}) = T(e_c) = 1 - \frac{1}{e_m^2}\left[e_m - 1 + \frac{a}{\sigma_p}\sqrt{\frac{\rho_w g E h}{12}}\right]^2, \quad 0 \leq e_c \leq e_m \quad \& \quad 0 \leq e_m < 1. \tag{6}$$

If the buckling event does not limit the load, then the local crushing event will limit it, thus

$$p(\text{crushes}) = 1 - p(\text{buckles}) \tag{7}$$

For a force chain having n contact interfaces, it is assumed that the load limit is reached when the system buckles or when any of the contact interfaces locally crushes. If n contact interfaces are assumed independent of each other and the local crushing assumed to not occur, the probability for buckling reads

$$p_n(\text{buckles}) = \prod_{i=1}^{n} p(\text{buckles}) = p(\text{buckles})^n. \tag{8}$$

The probability that a crushing event will limit the load is given by a complement probability of the previous equation reading

$$p_n(\text{crushes}) = 1 - p_n(\text{buckles}). \tag{9}$$

A simple way to demonstrate how the above described limit load model works, and the parameter effects it yields, is to consider a hypothetical peak load event caused by a pair of blocks. In this hypothetical case, the probability of a buckling event reads

$$p_n(\text{buckles}) = \left[1 - \frac{a^2 \rho_w g E h}{12 \sigma_p^2}\right]^n. \tag{10}$$

This example demonstrates that the force chains formed by blocks originating from an ice sheet with low E and/or h are more prone to buckle than the chains with blocks originating from a sheet with high E and/or h. The model thus yields plausible results: Probability of buckling events in ice-structure interaction process increases when ice thickness decreases (Sanderson, 1988).

3. Results and Discussion

Figure 4a shows the maximum peak ice load F^p values (Figure 2a and b) from our FEM-DEM simulations. Additionally, it shows the mean F^p values with their standard deviations for the simulations of each set, S1…S7 (Table 2). While the F^p values from the simulations in a given set show scatter, the mean F^p values of the sets S1…S7 differed considerably, by up to about 500 %, mainly due to a difference in ice thickness h between the sets(Ranta et al., 2017b). The simulations of set S7 with high σ_p yielded larger values than sets S5 and S6 with the same ice thickness $h = 1.25$ m. The values of a, solved by normalizing the F^p data of Figure 4a by factor $\sqrt{kEI}$, are shown in Figure 4b. These indicate that the peak load events were related to buckling: All mean values of a are in the same range and there is no dependency between a and h. Nonetheless, the data shows scatter not explained by the buckling model as, for example, the mean a value is clearly larger for set S7 having high σ_p.

The values of a for S7 are ideal for defining distribution for a to be used in the probabilistic limit load model (Equation 4), as they most likely are relates to the ice failure due to buckling, not by local ice crushing. Figure 5a shows a histogram for F^p observations of set S7. The figure also shows, and specifies, a two-parameter Gumbel distribution fitted to the a data. Figure 5b shows the data quantiles from the same data plotted against Gumbel theoretical quantiles, with the linearity of the data points showing that the Gumbel distribution describes the data well.

By utilizing the a value distribution related to simulation set S7, the use probabilistic limit load model can be demonstrated. This is here done using Figure 6a-d, which shows the probabilities p_n(buckles) and p_n(crushes) of buckling or local crushing failure (Equations 8 and 9), respectively, limiting the peak ice load F^p value. Figures 6a and b show p_n(buckles) and p_n(crushes) as a function of h with $\sigma_p = 1$ MPa. Figures 6c and d, on the other hand, show them plotted against σ_p with $h = 1.25$ m. All figures show the results for the number of ice floe contact interfaces $n = 4$ and 8. Figures 6a and b (similarly to c and d) differ by the value of e_m, the maximum contact offset, which was 0.6 and 0.8, respectively. Here a was fixed to 0.39 after the data for simulation set S7 (Figure 6b), while the other parameters were from Table 1.

Figures 6a-d show that the probabilistic limit load model yields, not only some fairly intuitive results, but also some less intuitive ones. The probability p_n(buckles) of buckling increases with σ_p and decreases with an increasing h. The first result is due to a high σ_p inhibiting the local crushing, while the latter can be understood by accounting for the buckling load being dependent on h. For a fixed σ_p, number of contact interfaces n has no effect on the limit for h, at which the peak load becomes solely governed by buckling. For example, when $\sigma_p = 2$

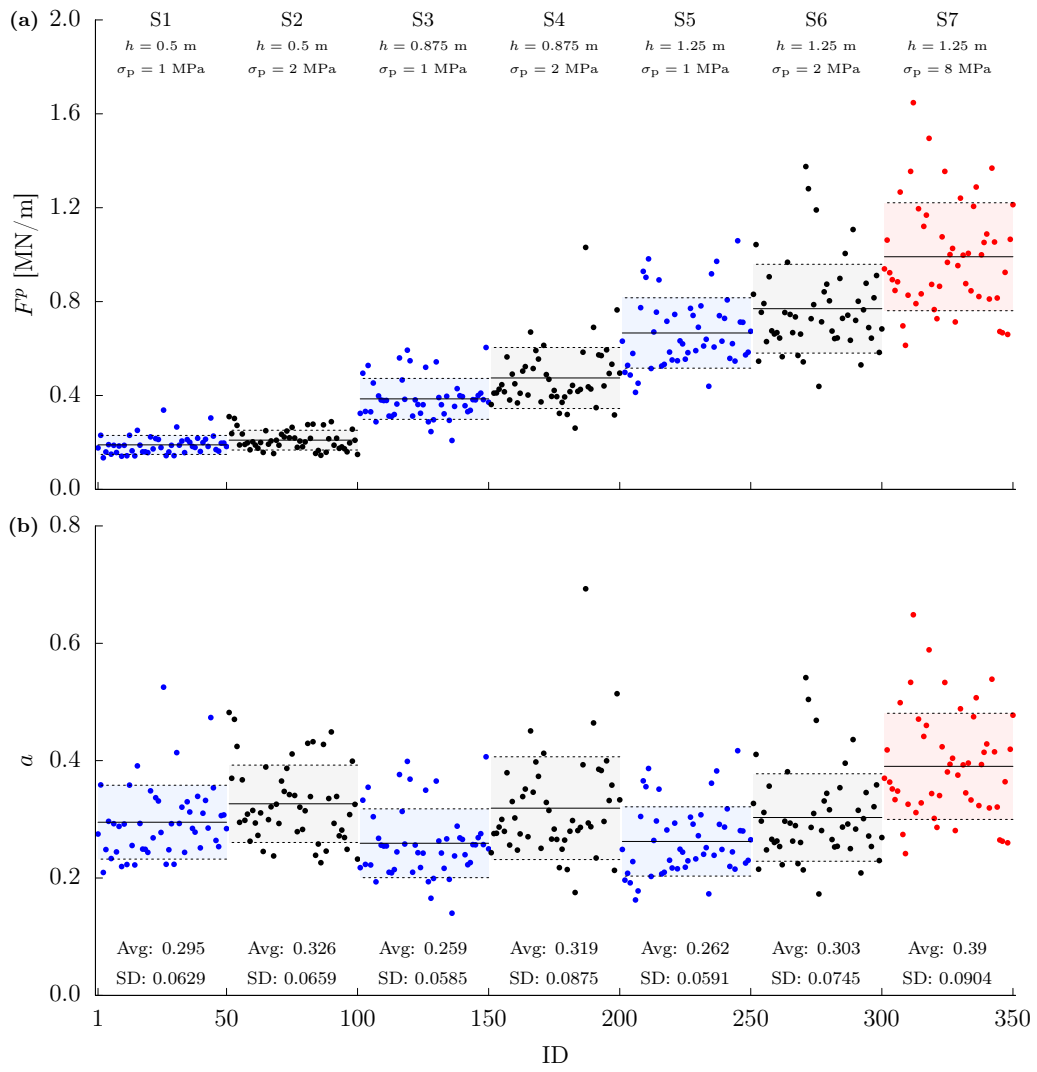

Figure 4: The values of (a) maximum peak ice load F^p values from all simulations (sets S1 . . . S7, Table 2) and (b) dimensionless a factors derived using F^p data. The graphs show the mean values (Avg, solid lines) and standard deviations (SD, dashed lines) for the data. The mean a value 0.39 of set S7 was used in plotting Figure 6

MPa, p_n(crushing) vanishes with $h < 0.4$ m for both n. Further, p_n(buckles) for fixed h or σ_p is seen to decrease when n increases. This underlines the importance of understanding local phenomena at the contact interfaces; the effect of local crushing may override the larger scale phenomena of force chain buckling, which is easier to detect.

Figures 6c and d show an important outcome of the model: For a fixed h, soft ice (low σ_p) will never fail by buckling. For example, in the case of the figures, where $h = 1.25$ m, the p_n(buckles) = 0 for $\sigma_p < 1$ MPa. This means that soft ice will never exhibit any failure mode other than local crushing and that, consequently, (1) the mechanical phenomena limiting F^p values in ice-structure interaction differs drastically for soft and strong ice and (2) the analysis of ice loading processes should account for this fact. We note that the values chosen for the maximum contact offset and number of contact interfaces, e_m and n, respectively, have only a very small effect on this observation.

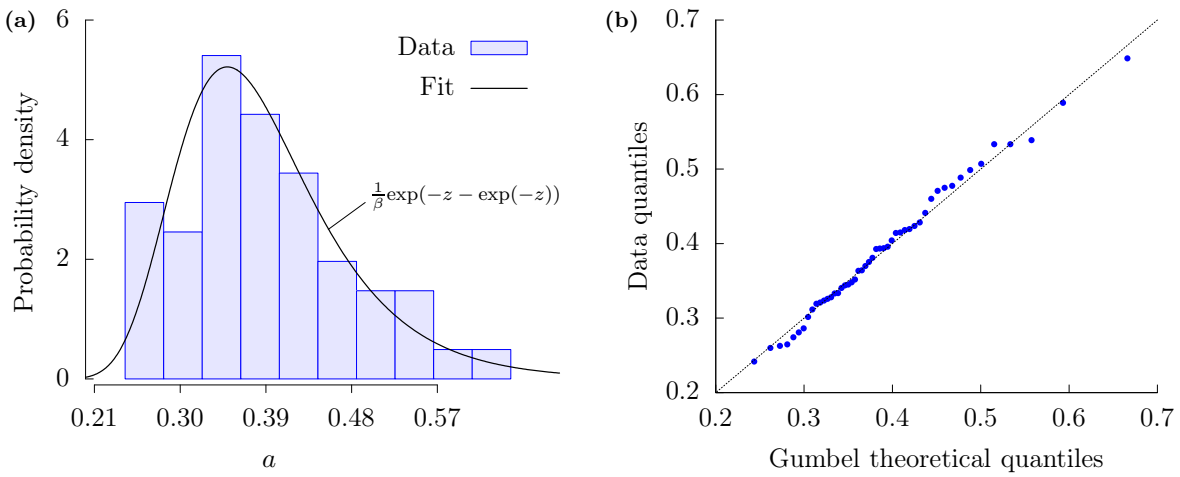

Figure 5: Distribution of a values for set S7 (ice thickness h = 1.25 m and high crushing strength σ_p = 8 MPa): (a) histogram with fitted Gumbel distribution and (b) data quantiles plotted against the Gumbel theoretical quantiles. The Gumbel distribution with $z = (a - \mu)/\beta$ had estimated parameter values $\mu = 0.3495$ and $\beta = 0.0705$.

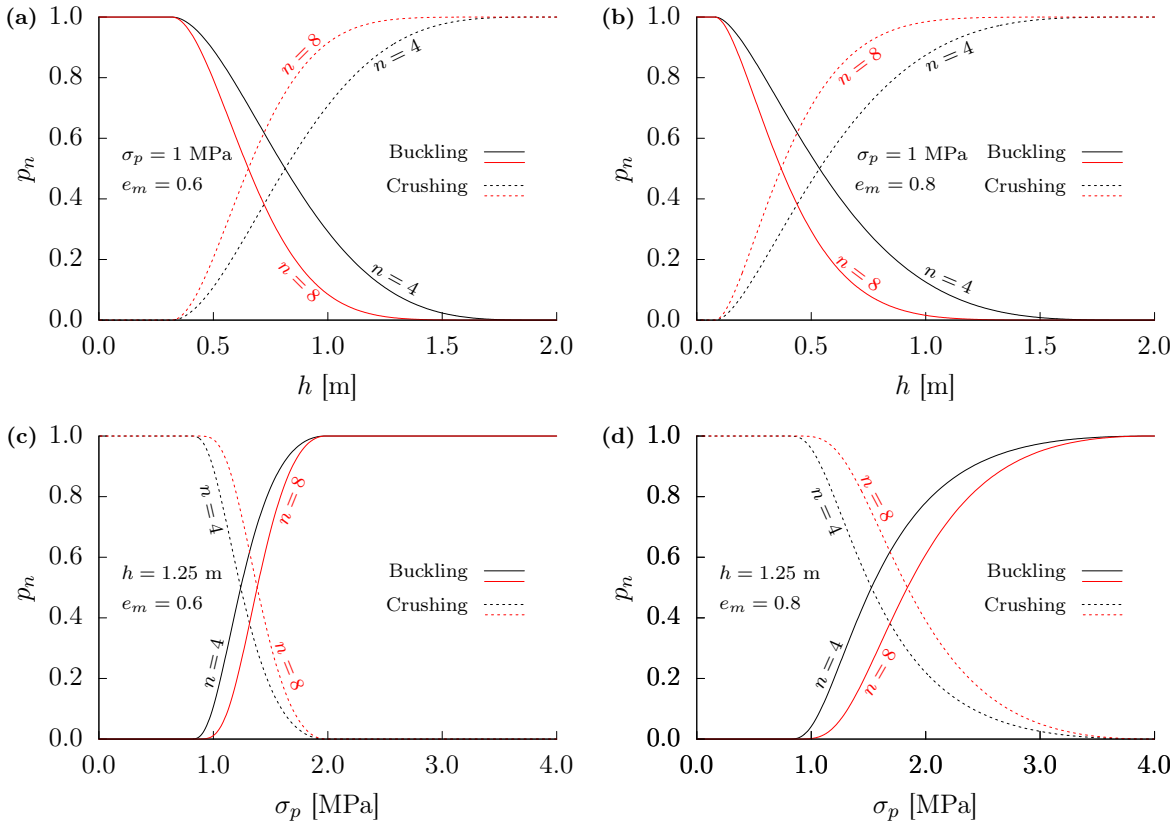

Figure 6: Probabilities p_n(buckles) and p_n(crushes) for buckling and local crushing events, respectively (Equations 8 and 9): (a) and (b) show p_n(buckles) and p_n(crushes) against ice thickness h for crushing strength σ_p 1 MPa and maximum contact offsets e_m = 0.6 and 0.8, respectively, and (c) and (d) as a function of σ_p for h = 1.25 m and e_m = 0.6 and 0.8, respectively. Parameter a was fixed to 0.39, which is the mean value of simulation set S7 (Figure 4b). Graphs show curves for two different number of contact interfaces n.

4. Conclusions

This paper introduced a probabilistic limit load model, which can be used in the analysis of peak ice load events on an inclined offshore structure. The model is based on simple mechanical

principles, and it accounts for a mixed-mode ice failure process where the root cause of ice failure can be due to either ice buckling or local crushing. Here we only briefly described the model and demonstrated its use, but more details can be found from Ranta and Polojärvi (2019), where the model is extended into an algorithm, capable of producing large amounts of virtual ice load data that compares fairly well with full-scale observations. The probabilistic limit load model has potential of yielding insight for the analysis of complex ice-structure interaction processes.

Acknowledgments

We are grateful for financial support from the Academy of Finland research projects (309830) Ice Block Breakage: Experiments and Simulations (ICEBES).

References

Daley, C., Tuhkuri, J., Riska, K., 1998. The role of discrete failures in local ice loads. Cold Regions Science and Technology 27, 197 – 211.

Hopkins, M., 1992. Numerical Simulation of Systems of Multitudinous Polygonal Blocks. Technical Report 92-22. Cold Regions Research and Engineering Laboratory, CRREL. 69 p.

Jordaan, I., 2001. Mechanics of ice-structure interaction. Engineering Fracture Mechanics 68, 1923–1960.

Paavilainen, J., Tuhkuri, J., 2012. Parameter effects on simulated ice rubbling forces on a wide sloping structure. Cold Regions Science and Technology 81, 1–10.

Paavilainen, J., Tuhkuri, J., Polojärvi, A., 2009. 2D combined finite–discrete element method to model multi-fracture of beam structures. Engineering Computations 26, 578–598.

Ranta, J., Polojärvi, A., 2019. Limit mechanisms for ice loads on inclined structures: Local crushing. Submitted to Marine Structures .

Ranta, J., Polojärvi, A., Tuhkuri, J., 2017a. Sources of stochasticity in ice-structure interaction process, in: Proceedings of the 24th International Conference on Port and Ocean Engineering under Arctic Conditions, POAC'17, Busan, Korea (electronic publication).

Ranta, J., Polojärvi, A., Tuhkuri, J., 2018a. Limit mechanisms for ice loads on inclined structures: Buckling. Cold Regions Science and Technology 147, 34–44.

Ranta, J., Polojärvi, A., Tuhkuri, J., 2018b. Scatter and error estimates in ice loads—Results from virtual experiments. Cold Regions Science and Technology 148, 1–12.

Ranta, J., Tuhkuri, J., Polojärvi, A., 2017b. The statistical analysis of peak ice loads in a simulated ice-structure interaction process. Cold Regions Science and Technology 133, 46–55.

Sanderson, T., 1988. Ice Mechanics, Risks to Offshore Structures. Graham & Trotman Inc. Kluwer Academic Publishers Group.

Schreyer, H., Sulsky, D., Munday, L., Coon, M., Kwok, R., 2006. Elastic-decohesive constitutive model for sea ice. Journal of Geophysical Research: Oceans 111.

Timco, G., Weeks, W., 2010. A review of the engineering properties of sea ice. Cold Regions Science and Technology 60, 107–129.